FORCE LIMITS FOR VIBRATION TESTS

Terry D. Scharton

Jet Propulsion Laboratory
California Institute of Technology
Pasadena, CA, 91109-8099, USA

ABSTRACT *- The theoretical basis of force limited vibration testing is reviewed, the results of a frequency shift method of deriving force limits are presented, and two recent applications of the technique are described.*

1- INTRODUCTION

A new vibration testing technique, which limits the force applied to the test item by the shaker, has been used successfully in more than ten JPL flight project vibration tests during the past four years [Scharton 93]. For lightweight aerospace structures, the mechanical impedance of the test item and the flight mounting structure are typically comparable so that the combined motion involves modest interface forces and little amplification. Thus the high amplification resonances and associated failures which occur in conventional vibration tests, with essentially unlimited force, are test artifacts which can be eliminated by limiting the force in the test to that predicted for flight. Input force limiting is in theory equivalent to response limiting, but force limiting is often more convenient (critical response locations are sometimes numerous and not accessible) and less dependent on the details of payload models. Implementation of force limiting requires: derivation of a force specification (analogous to that for acceleration), a vibration test fixture to accommodate force sensors, and shaker operation with dual control of both acceleration and force.

2- THEORETICAL BASIS

The process of deriving an acceleration specification for a vibration test is illustrated in Fig. 1. The ragged curves in Fig. 1 are random vibration measurements at the interface between electronic boxes and the supporting honeycomb panels in the TOPEX/Poseidon spacecraft acoustic test [Boatman 92]. Also shown is the random vibration test specification used previously to qualify the boxes. The vibration test specification is a reasonably good envelope of the test data in the mid-frequency range. (The random vibration specification also covers structureborne vibration at the low frequencies and direct acoustic excitation at the high frequencies, and these environments are not reflected in the acoustic test interface vibration data shown in Fig. 1.) The highlighted data in Fig. 1 show that the notches in the interface acceleration, most of which occur at load antiresonance frequencies, are lost in this enveloping process, The load is very responsive at the

antiresonance frequencies and acts as a dynamic absorber to notch the input. Ignoring the notches in the acceleration input results in overtesting in conventional vibration tests by typically 10 dB to 20 dB. In force limited vibration tests, both the interface acceleration and force are controlled. The reaction forces at the load antiresonance frequencies are limited to values predicted for the flight mounting configuration, and the notches in the input acceleration are automatically restored.

Equation 1, which may be derived from Norton's and Thevenin's equivalent circuit theorems, provides a theoretical basis for dual control of force and acceleration in vibration tests:

$$1 = A/Ao + F/Fo \qquad (1)$$

where: A is the interface acceleration, Ao is the source free acceleration, F is the interface force, and Fo is the source blocked force [Scharton 90]. Equation 1 is exact but difficult to apply because each term is a complex function of frequency, and phase is ignored in current vibration test controllers. An approximate form of eq. 1 useful for control of vibration tests is the extremal control equation:

$$|A| \leq |As|, \text{ and } |F| \leq |Fs| \qquad (2)$$

where the free acceleration and blocked force are replaced by specifications which envelope the interface values in the coupled system [Murfin 68, Scharton 90, & Smallwood 90]. Most vibration controllers have the capability for extremal control, that is, to select the larger of t wo or more feedback signals in each narrow frequency analysis band for control to a vibration specification. However, older controllers allow only one specification. In this case to implement dual control, a filter must be used to scale the shaker force control signal to an equivalent acceleration, New controllers allow separate specifications for response control channels so that Eq. 2 maybe implemented without any complications.

3 - DERIVATION OF FORCE SPECIFICATIONS

There are virtually no flight data and little system test data on the vibratory forces at mounting structure and test item interfaces. Force limits for vibration tests are therefore currently derived using analytical or measured structural impedances of the mounting structure and the test items, together with the interface acceleration specification. Herein a "frequency shift method' [Scharton 94] of calculating the force limits is applied to a simple and to a complex two-degree-of-freedom system (TDFS).

Consider the simple TDFS shown in Fig. 2. The two oscillators represent coupled resonant modes of the source and load in each frequency band, e.g. one-third octave bands, so the oscillator masses M_1 and M_2 are dependent on frequency. For the simple TDFS, the maximum interface force and maximum response of the load occur when the resonance frequency of the load equals that of the source [Crandall 73]. For this case, the characteristic equation is that of a classical dynamic absorber [Den Hartog 47]:

$$(w/w_o)^2 = (1 + u/2) * (U + u^2/4)^{0.5} \quad (3)$$

where: w_o is the resonance frequency of the individual oscillators and u is the ratio of load to source masses (M_2/M_1). Both the interface force (F) and acceleration (A 1) spectral densities have maxima at the coupled system resonance frequencies, and the ratio of the maxima is calculated from the magnitude squared of the load dynamic mass, which for the simple TDFS in Fig. 2 is:

$$S_{ff}/(S_{aa} M_2^2) = [1 + (w/w_o)^2 / Q^2] / \{[1 - (w/w_o)^2]^2 + (w/w_o)^2 / Q^2\} \quad (4)$$

where Q is the quality factor, the reciprocal of twice the critical damping ratio, of the load.

The ratio of normalized force to acceleration spectral density at the coupled system resonances is obtained by combining Eqs. 3 and 4. The ratio of normalized force to acceleration is slightly larger at the lower resonance frequency of Eq. 3, and the ratio for that case is plotted in Fig. 2 against the mass ratio (M_2/M_1) for three values of Q. For very small (0.0001) values of the load to source mass ratio, the load has no effect on the source and the peak amplification factor is Q squared, For larger ratios of the mass ratio, there is less amplification because of the previously discussed notching at the load antiresonance frequencies. When the load and source masses are comparable, which is common in aerospace structures, there is little amplification between the source and the load for the simple TDFS.

In most previous JPL force limited vibration tests, the oscillator masses in Fig. 2 have been taken as the residual masses (the sum of the effective masses of all modes with resonances above the excitation frequency) from finite-element-method (FEM) analyses, or alternately as the smoothed frequency response function (FRF) of the ratio of drive point force to acceleration, measured with a shaker or impact hammer. Defining the oscillator masses as the residual masses is conservative for qualification, However, the single mass models of the source and load in Fig. 2 have inherent conceptual difficulties and are limited in their capability to accurately represent the force contributions of both resonant and nonresonant modes.

Figure 3a shows a model of a source and load in which each mode maybe represented as a single-degree-of-freedom system attached to the connection interface. (This is sometimes called an asparagus patch model.) Derivation of this type of model from a FEM analysis requires normalizing the modes so that the reaction forces equal the inertial forces [Wada 72]. When this model is excited at the interface at a frequency near the resonance frequency w_n of the n^{th} mode, the model may be simplified to that in Fig, 3b, where m_n is the modal mass of the n^{th} mode and M_n is the residual mass, i.e. the sum of the masses of the n^{th} and all higher resonance frequency modes. A more complex TDFS is obtained by connecting the residual masses of a source and load models like that in Fig. 3b. (The rigid body translation mode is ignored.) In order to eliminate the afore mentioned limitations of the simple TDFS analysis, the frequency shift method has recently been applied to this more complex TDFS [Scharton 94].

The ratio of the normalized force spectral peak to the acceleration spectral peak is calculated for the complex TDFS as for the simple TDFS, except that there are two complications First for the complex TDFS, the force and acceleration do not always peak at the same resonance frequency so it is necessary to calculate the mode shapes in order to get the ratio of the bigger force peak to the bigger acceleration peak. (It is desired to envelope both the force and acceleration,) Second, the greatest ratio of force to acceleration does not always occur at a single ratio of load to source resonance frequencies, so it is necessary to conduct a tuning analysis,

The ratios of the normalized force spectral peak to the acceleration spectral peak for the complex TDFS are listed in Table 1 for a load amplification factor Q_2 of 20. (Results for other Q's are available from the author.) The maximum normalized forces are rounded to whole numbers. The ratio of load to source resonance frequency squared in 16ths, which resulted in the maximum normalized forces, are identified by the digits to the right of the decimal in Table 1. The results are similar to those for the simple TDFS in Fig, 2 except that at large values of the mass ratio, the normalized force tends to be larger than unity for the complex TDFS.

4- APPLICATION ONE -- WFPC 11 FOR HUBBLE TELESCOPE

The Wide Field Planetary Camera 11 (WFPC 11) installed in the Hubble Telescope during the first servicing mission in December 1993, was subjected to a vertical axis protoflight level random vibration test at JPL as shown in Fig. 4. A large (approx. 10 cm diam.) commercially available triaxial force transducer was located just below each of the three latches which attach the camera to the telescope. After the first low level random run, it was determined that three of the four control channels available on the older vibration controller were essential to control the high frequency acceleration input at each of the three latches, so only one control channel was available for force limiting. (New controllers have 8 to 64 control channels.) On the basis of analysis and the low level data, it was decided to limit only the vertical force at the A latch (at the far left in Fig. 4) which reacts most of the loads because of the outboard (to the right in Fig. 4) center of gravity of the camera. The effective mass of the source was determined from modal hammer tests of the honeycomb container (the radial SIPE) which housed the WFPC 11 in the Space Shuttle; the measured effective mass at the A latch location on the container in the vertical direction is shown in Fig. 5. Three components of force at each of the three WFPC 11 latches were recorded and analyzed in a low level sine test immediately preceding the random vibration test; the measured effective mass at the A latch of the WFPC 11 in the vertical direction is shown in Fig. 6.

The acceleration measured at each of the three latches is compared with the acceleration specification for the protoflight random vibration test in Fig, 7, and the vertical force measured at each of the three latches is compared to the vertical force specification for the A latch in Fig. 8. The A latch vertical force specification for the random vibration test was determined using the simple TDFS curves of Fig. 2 as follows. The effective mass of the WFPC II at 100 Hz from Fig. 6 is 33 kg. or 73 lbs and that of the container from Fig, 5 is 100 kg. Therefore the mass ratio is 1/3 and the force spectrum is calculated from Fig. 2 as approximately 500 lbs^2/Hz for an acceleration specification of 0.02 G^2/Hz at 100 Hz,

Comparison of Figs. 7 and 8 shows that limiting the A latch vertical force resulted in notching of the acceleration input at 35 Hz, 100 Hz and 150 Hz. (The acceleration notch at 70 Hz was effected by artificially reducing the A latch vertical force specification at 70 Hz for a mode which only showed up in the A latch transverse force, which was not in the control loop.) Above 300 Hz, one of the three control accelerometers is at the specification at every frequency.

S - APPLICATION TWO -- RPWS ANTENNAS FOR CASSINI SPACECRAFT

Figure 9 shows the engineering model of the Radio Plasma Wave Search (RPWS) antenna assembly for the Cassini spacecraft mounted for a lateral random vibration test. Small, approximately 2.5 cm. square, triaxial force gages are located between the RPWS assembly and the vibration test fixture at each of the three attachment points. Neither modal tap test data nor FEM information on the effective mass of the spacecraft were available to calculate a force specification. Therefore the mounting structure effective mass was taken as the magnitude of the drive point impedances of simple infinite beam models of the spacecraft ring frames to which the RPWS assembly are attached. Force limits were calculated using both the simple TDFS results in Fig, 2 and the complex TDFS results in Table 1, and the two calculations are shown in Fig. 10. The force specification used in the testis a generous envelope of both calculations, because of the crude estimate of the mounting structure effective mass and in order to insure that engineering model test is more conservative than later flight hardware tests. Fig. 11 compares the measured lateral in axis forces in an 18 dB down random vibration test without force limiting with the scaled down force specification. Fig 12 shows the notched acceleration input in the full level random vibration test with force limiting. The notches in the acceleration input are essentially mirror images of the force exceedances in Fig. 11.

6- CONCLUSIONS

Force limiting has been used successfully in over ten flight project vibration tests at JPL during the past four years. Force limiting minimizes the risk of overtesting and the associated failures, cost penalties, and schedule delays. In addition, more and better science can be flown for fixed costs, because the hardware need not be over designed for artificial tests. Analytical techniques are available to predict the vibratory flight force limits based on the acceleration specification and measurements or analyses of the mounting structure and test item mechanical impedances. Triaxial force gages and associated signal conditioning to measure the forces in vibration tests are commercial y available. The new vibration controllers, with the capability for multiple reference specifications for response limiting, can be conveniently used for force limiting. In spite of the many successful applications of force limiting, a number of interesting research problems remain. Some problems of current interest are: obtaining flight vibratory force data for validation of the technique, calculating and measuring moment impedances, combining multipoint impedances, and assessing errors associated with force measurements.

7- ACKNOWLEDGEMENTS

l'he author wishes to acknowledge Allan Piersol of Piersol Engineering Inc., David Smallwood at Sandia National Laboratory, and Bob Bamford and other colleagues at JPL for their help in the development and application of this technology. Thanks are also due to NASA Headquarters Office of Safety and Mission Assurance for funding the development of NASA guidelines and standard practices for force limited vibration testing. The work described in this paper was carried out by the Jet Propulsion Laboratory, California Institute of Technology under a contract with the National Aeronautics and Space Administration.

REFERENCES

T. Scharton, "Force Limited Vibration Testing at JPL", Proceedings of the 14th Aerospace Testing Seminar, Aerospace Corp., Manhattan Beach, Ca. March 1993.

D. Boatman, T. Scharton, D. Hershfeld, and P. Larkin, "Vibration and Acoustic Testing of TOPEX/Poseidon Spacecraft", 17th Space Simulation Conference Terrestrial Test for Space Success, NASA Conference Publication 3181, Baltimore Md, Nov. 1992.

T, Scharton, "Analysis of Dual Control Vibration Testing", Institute of Environmental Sciences Annual Meeting, San Diego, CA., 1990

W, Murfin, "Dual Specification in Vibration Testing", Shock and Vibration Bulletin, No 38, Part 1, August 1968

T. Scharton, "Force Specifications for Extremal Dual Controlled Vibration Tests", 61st Shock and Vibration Bulletin, Los Angeles, CA, October 1990.

D. Smallwood, "Development of the Force Envelope for an Acceleration/Force Extremal Controlled Vibration Test", 61st Shock and Vibration Bulletin, Los Angeles, CA, October 1990.

T. Scharton, "Vibration Test Force Limits Derived From Frequency Shift Method", 35th AIAA Structures, Structural Dynamics, and Materials Conference, Hilton Head, SC, April 18-20, 1994.

S. Crandall and W. Mark, RANDOM VIBRATIONS IN MECHANICAL SYSTEMS, Academic Press, N. Y., 1973, pp. 138 and 139.

J. Den Hartog, MECHANICAL VIBRATIONS, Mcgraw-Hill Co., NY, 1947, p. 115.B.

Wada, R. Bamford, and J. Garba, "Equivalent Spring-Mass System: A Physical System", 42nd Shock and Vibration Bulletin, 1972.

Table Y: Force Limit Spectrum Normalized by Acceleration Specification Spectrum and Load Weight Squared, Calculated From Complex TDFS For Q_2=20 (Decimal indicates in sixteenths the ratio of load to source resonance frequency squared from tuning analysis.)

Fig. 1: Electronic Box and Honeycomb Panel Interface Random Vibration Data in TOPEX/Poseidon Spacecraft Acoustic Test

Fig. 2: Normalized Force Limit Spectrum Calculated from Simple TDFS

Fig. 3a: Asparagus Patch Oscillator Model of Source or Load

Fig, 3b: Residual and Modal Mass Model of Source or Load

Fig. 4: Hubble Telescope WFPC II Vertical Random Vibration Test

Fig. 5: Effective Mass of WFPC II Container Measured with Modal Hammer

Fig. 6: Effective Mass of WFPC 11 in Low Level Sine Vibration Test

Fig. 7: Acceleration Specification and Data for WFPC II Random Vibration Test

Fig. 8: Force Specification and Data for WFPC II Random Vibration Test

Fig. 9: Cassini RPWS Antenna Assembly Engineering Model in Lateral Random Vibration Test

Fig. 10: Lateral Force Specification for RPWS Antenna Assembly

Fig. 11: Comparison of Measured Force and Specification in RPWS Antenna Assembly Engineering Model -18 dB Random Vibration Test without Force Limiting

Fig. 12: Notched Acceleration Input in RPWS Antenna Assembly Engineering Model Protoflight Level Random Vibration Test with Force Limiting ‘

AMPLIFICATION FACTOR (Q)	20									
RESIDUAL MASS RATIO (M2/M1)		0.001	0.003	0.01	0.03	0.1	0.3	1	3	10
RATIO OF MODAL TO RESIDUAL MASS										
Source (m1/M1)	Load (m2/M2)									
1	1	359.32	283.32	166.32	100.31	50.3	34.27	26.24	23.23	23.22
1	0.7	187.32	157.32	102.32	64.31	34.3	21.28	17.24	15.22	14.22
1	0.5	100.32	89.32	63 .32	42.31	24.3	15 .28	1 2.24	11.22	11.21
1	0.3	39.32	37.32	30.32	22.31	14.3	9.28	7.25	6.22	7.2
1	0.1	6.33	6.33	6.32	5.33	4.32	4.28	3.26	3.22	3.2
AMPLIFICATION FACTOR (Q)	20									
RESIDUAL MASS RATIO (M2/M1)		0.001	0.003	0.01	0.03	0.1	0.3	1	3	10
RATIO OF MODAL TO RESIDUAL MASS										
Source (m1/M1)	Load (m2/M2)									
0.7	1	372.27	312.27	200.27	103.27	57.26	34.25	27.23	24.22	23.22
0.7	0.7	191.27	170.27	120.27	67.27	39.26	23.25	18.23	16.22	15.21
0.7	0.5	104.27	94.27	73.27	44.27	27.26	16.25	12.23	11.21	12.01
0.7	0.3	38.27	38.27	33.27	23.27	15.26	10.25	7.23	7.21	7.2
0.7	0.1	6.28	6.28	6.28	6.27	5.26	4.25	3.24	3.21	4.18
AMPLIFICATION FACTOR (Q)	20									
RESIDUAL MASS RATIO (M2/M1)		0.001	0.003	0.01	0.03	0.1	0.3	1	3	10
RATIO OF MODAL TO RESIDUAL MASS										
Source (m1/M1)	Load (m2/M2)									
0.5	1	377.24	319.24	211.24	117.24	59.23	39.23	27.22	24.22	22.22
0.5	0.7	193.24	172.24	125.24	74.24	39.23	25.23	19.22	15.22	15.21
0.5	0.5	102.24	95.24	7●24	48.24	27.23	17.23	12.22	11.21	12.01
0.5	0.3	39.24	38.24	33.24	24.24	15.23	10.23	8.21	8.2	7.2
0.5	0.1	6.25	6.24	6.24	6.24	5.24	4.23	3.22	4.19	4 18
AMPLIFICATION FACTOR (Q)	20									
RESIDUAL MASS RATIO (M2/M1)		0.001	0.003	0.01	0.03	0.1	0.3	1	3	10
RATIO OF MODAL TO RESIDUAL MASS										
Source (m1/M1)	Load (m2/M2)									
0.3	1	367.21	319.21	230.21	142.21	76.21	41.21	27.21	23.22	22.22
0.3	0.7	188.21	170.21	132.21	86.21	48.21	29.21	20.21	17.21	16.21
0.3	0.5	100.21	93.21	77.21	54.21	31.21	19.21	13.21	11.21	12.11
0.3	0.3	39.21	37.21	33.21	26.21	17.21	12.2	9.2	7.2	7.19
0.3	0.1	6.21	6.21	6.21	6.21	5.21	5.2	4.19	4.18	4.18
AMPLIFICATION FACTOR										
RE IDUAL MASS RAT 2/M										
RAT MODAL RESIDUAL MASS										
Source (m1/M1)	Load (m2/M2)									
0.1	1	343.18	320.18	271.18	209.18	94.18	46.19	28.21	24.21	22.22
0.1	0.7	174.18	166.18	146.18	117.18	70.18	37.19	21.2	16.21	15.21
0.1	0.5	93.18	89.18	81.18	68.18	50.18	23.18	15.19	12.2	11.2
0.1	0.3	36.18	36.18	34.18	30.18	24.18	17.18	9.19	8.19	8.19
0.1	0.1	6.18	6.18	6.18	6.18	5.18	5.18	4.18	4.18	3.19

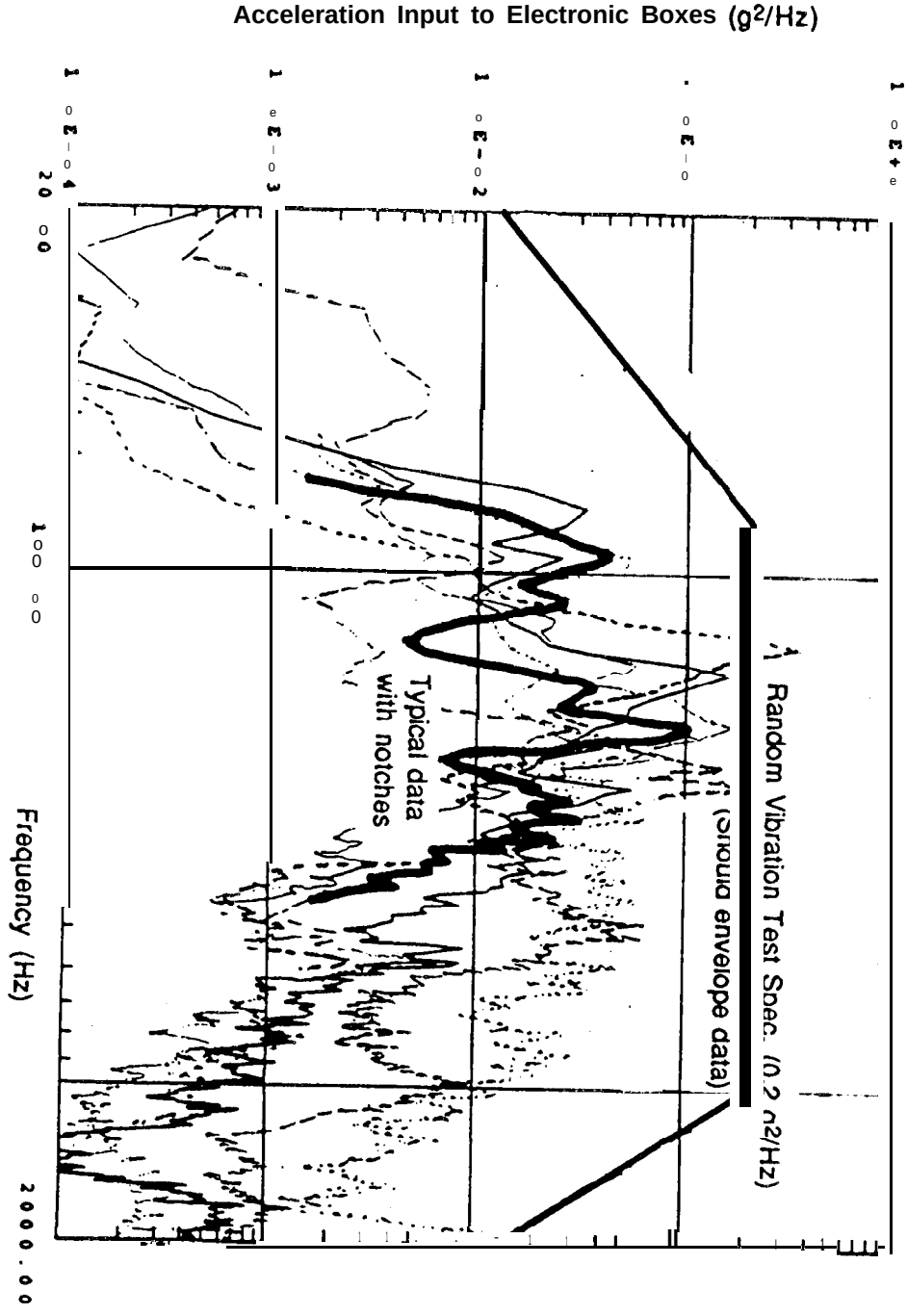
Acceleration Input to Electronic Boxes (g²/Hz)
1 E+0
1 E-0
1 E-02
1 E-03
1 E-04
20.00
100.00
2000.00
Frequency (Hz)
Random Vibration Test Spec. (0.2 g²/Hz)
(Should envelope data)
Typical data
with notches

Force Spectral Peak Normalized by Load Effective Mass
Squared and Acceleration Spectral Peak
Ratio of Load to Source Effective Mass (M2/M1)
0.0001
0.001
0.01
0.1
1
10
1
10
100
1000
10000
Q=5
Q=20
Q=50
Source
Load
Interface
Base Motion
External Force

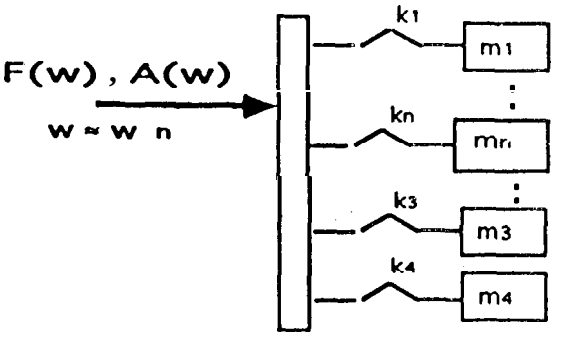

w 1, Stiffness Controlled Mode

wn , Resonant" Mode

w3
w4
} ,Mass Controlled Modes

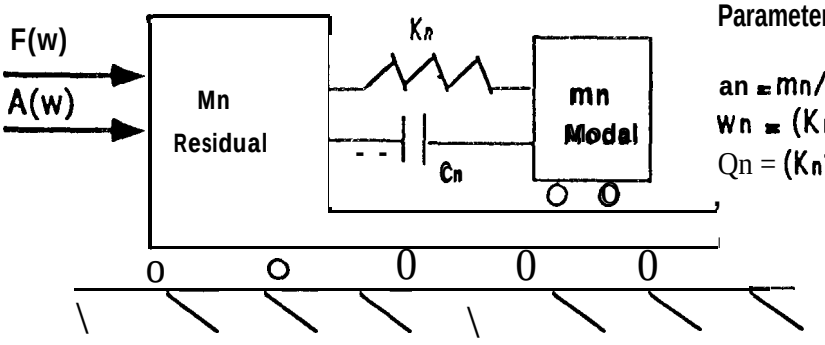

Parameters:

an = mn/Mn
wn = (Kn/mn)·5
Qn = (Kn*mn)·5/Cn

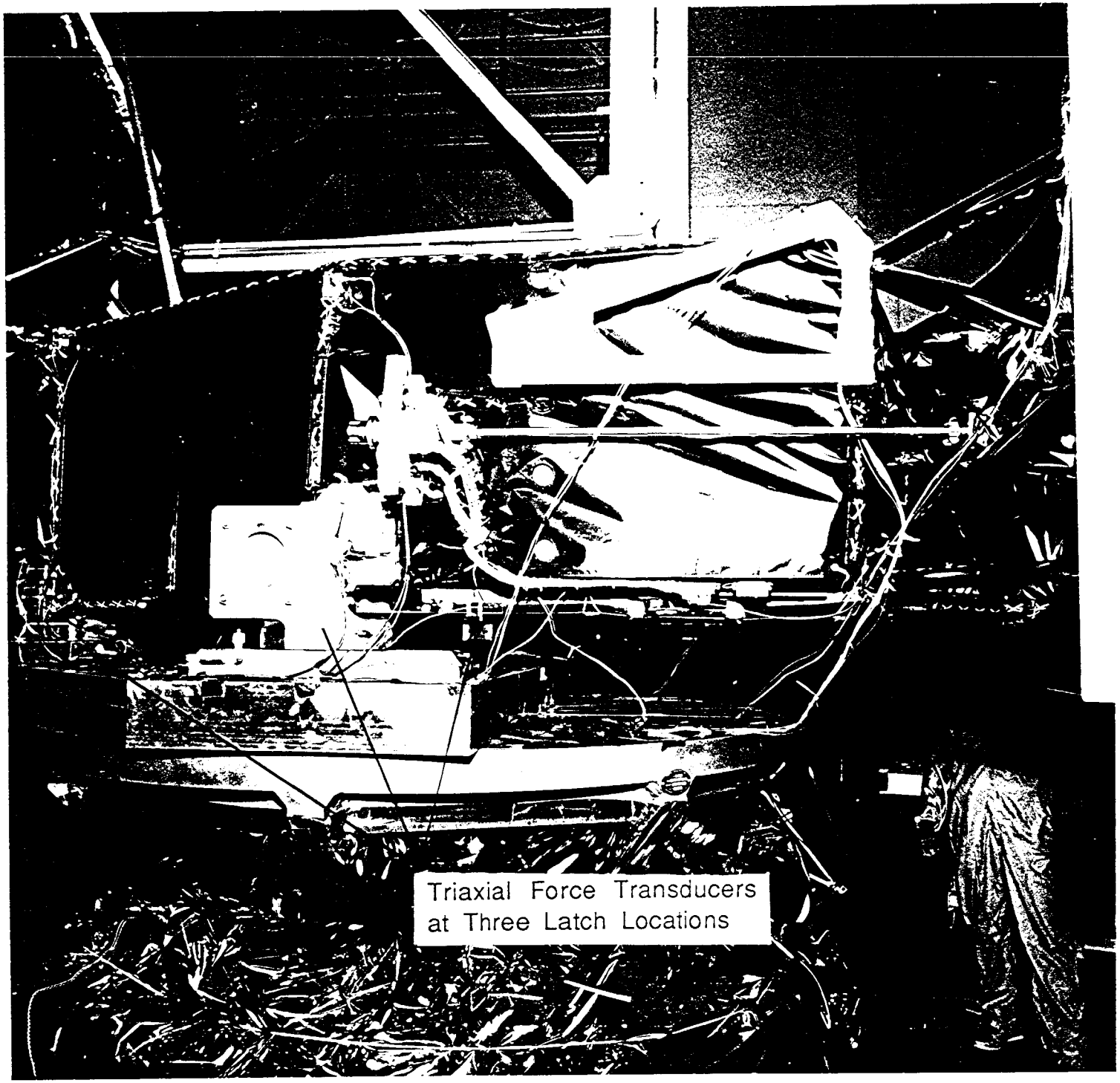
Triaxial Force Transducers
at Three Latch Locations

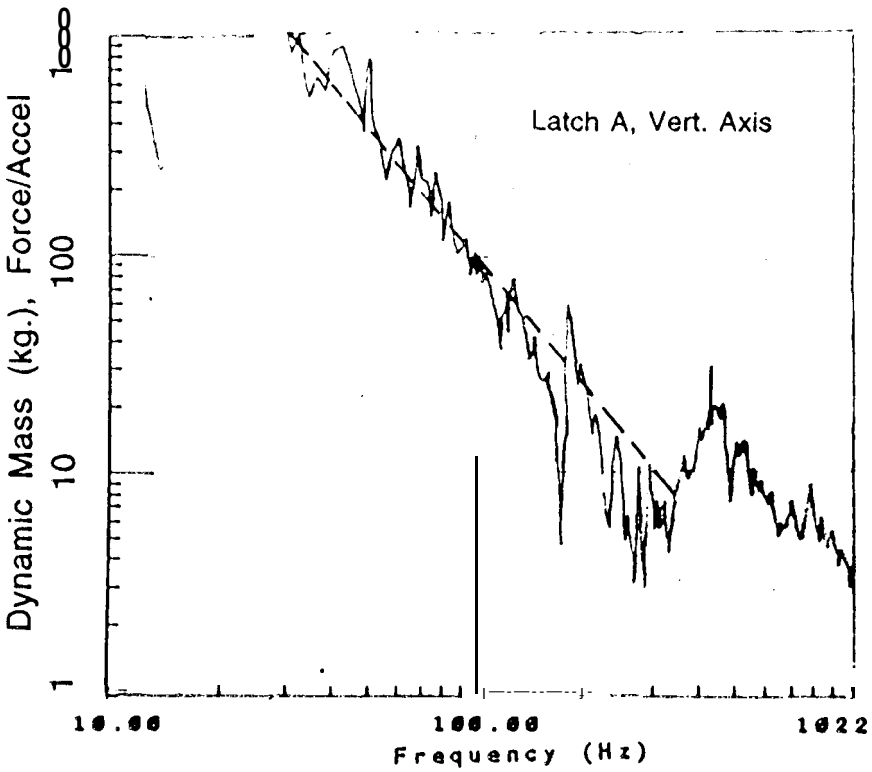
Latch A, Vert. Axis
Dynamic Mass (kg.), Force/Accel
1000
100
10
1
10.00
100.00
1022
Frequency (Hz)

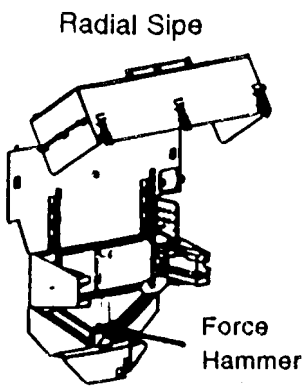
Radial Sipe
Force
Hammer

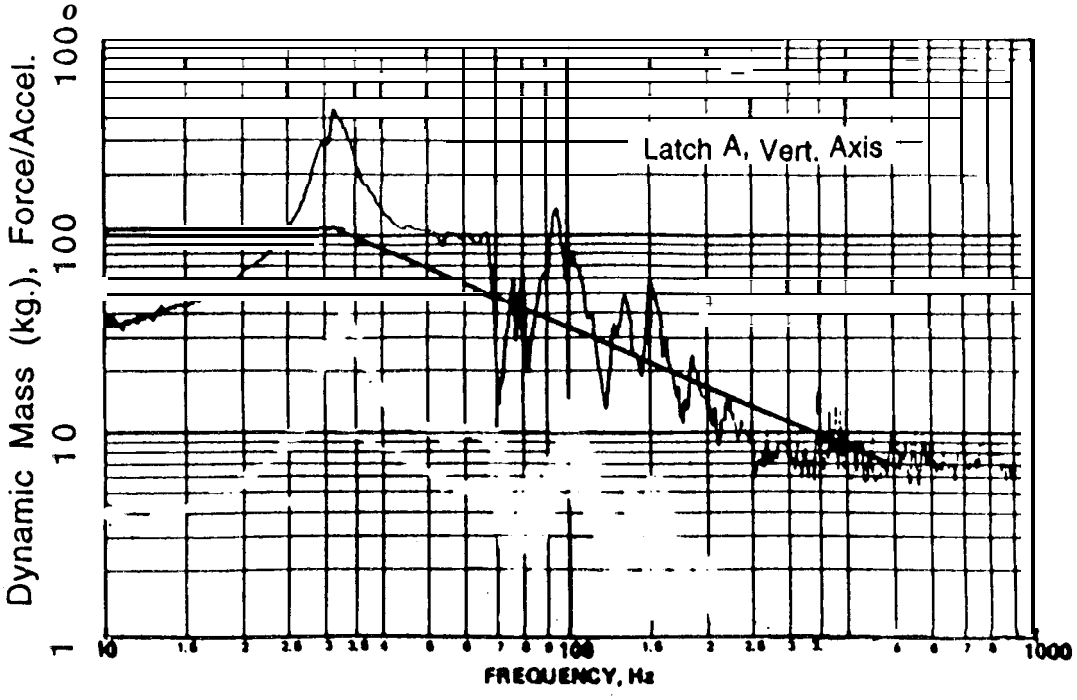
Latch A, Vert. Axis
Dynamic Mass (kg.), Force/Accel.
1000
100
10
1
10
100
1000
FREQUENCY, Hz

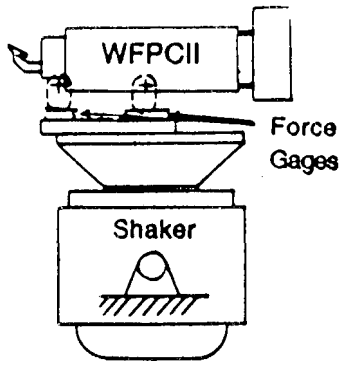
WFPCII
Force
Gages
Shaker

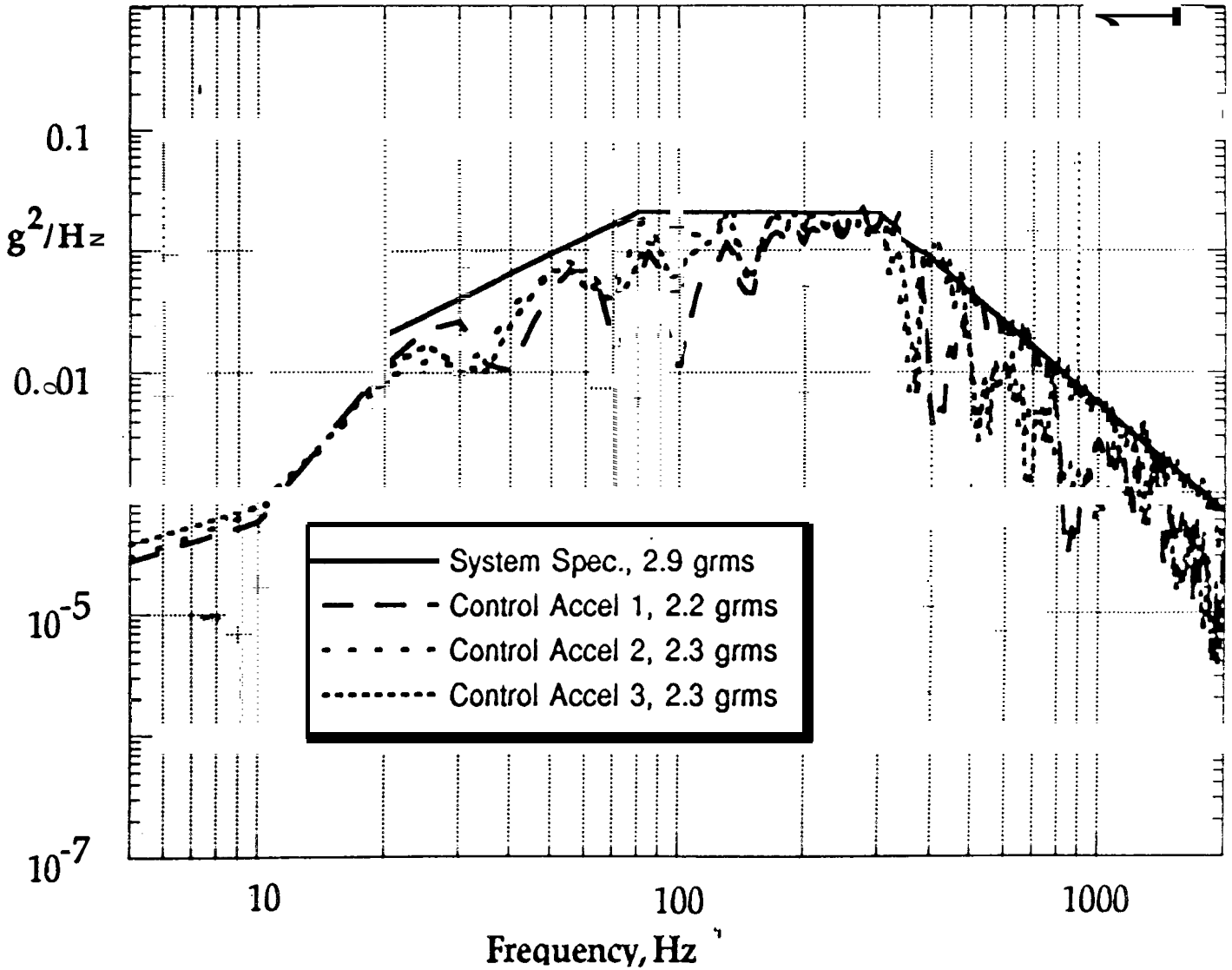
0.1
g²/Hz
0.01
10⁻⁵
10⁻⁷
10
100
1000
Frequency, Hz
System Spec., 2.9 grms
Control Accel 1, 2.2 grms
Control Accel 2, 2.3 grms
Control Accel 3, 2.3 grms

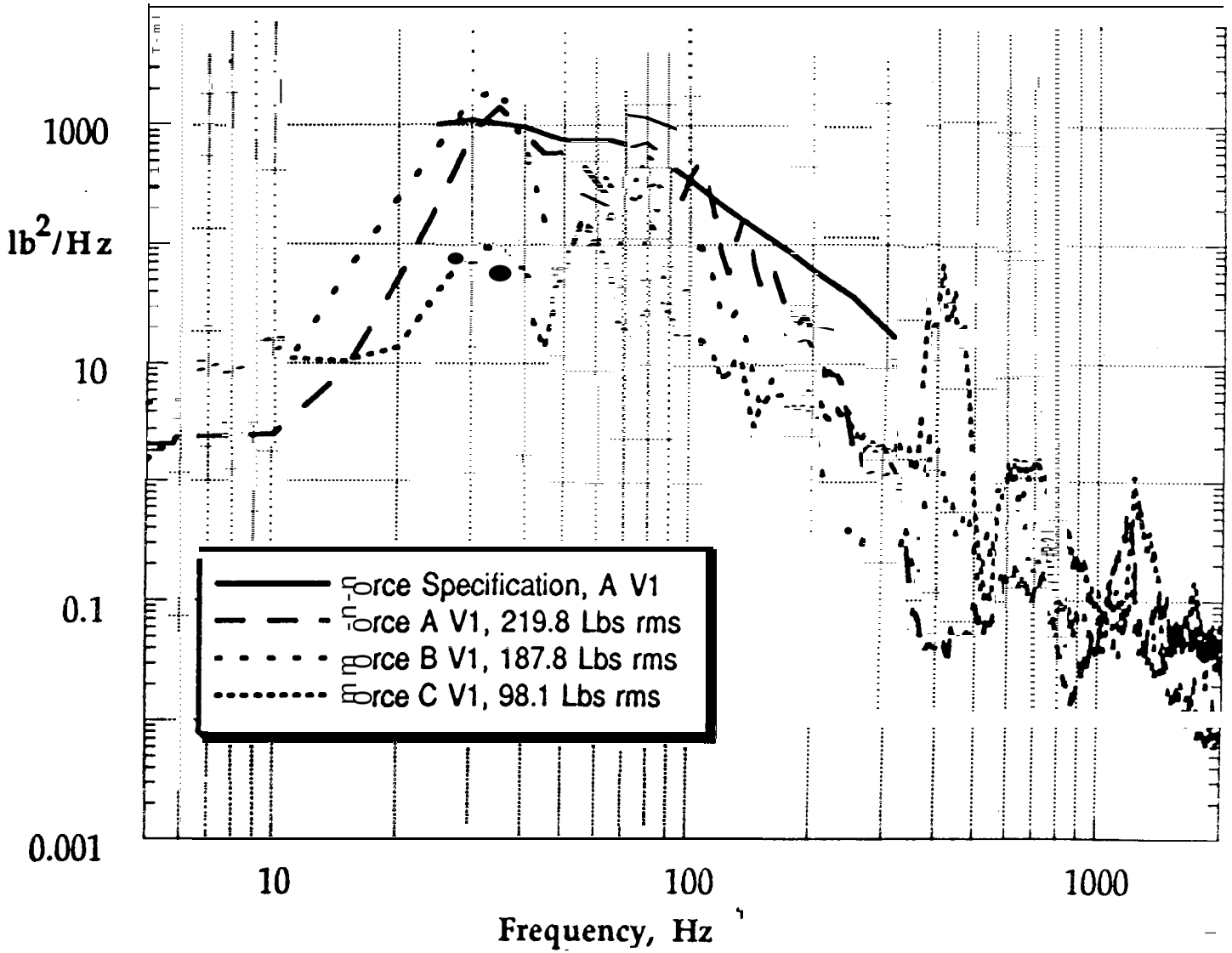
1000
lb²/Hz
10
0.1
0.001
10
100
1000
Frequency, Hz
Force Specification, A V1
Force A V1, 219.8 Lbs rms
Force B V1, 187.8 Lbs rms
Force C V1, 98.1 Lbs rms

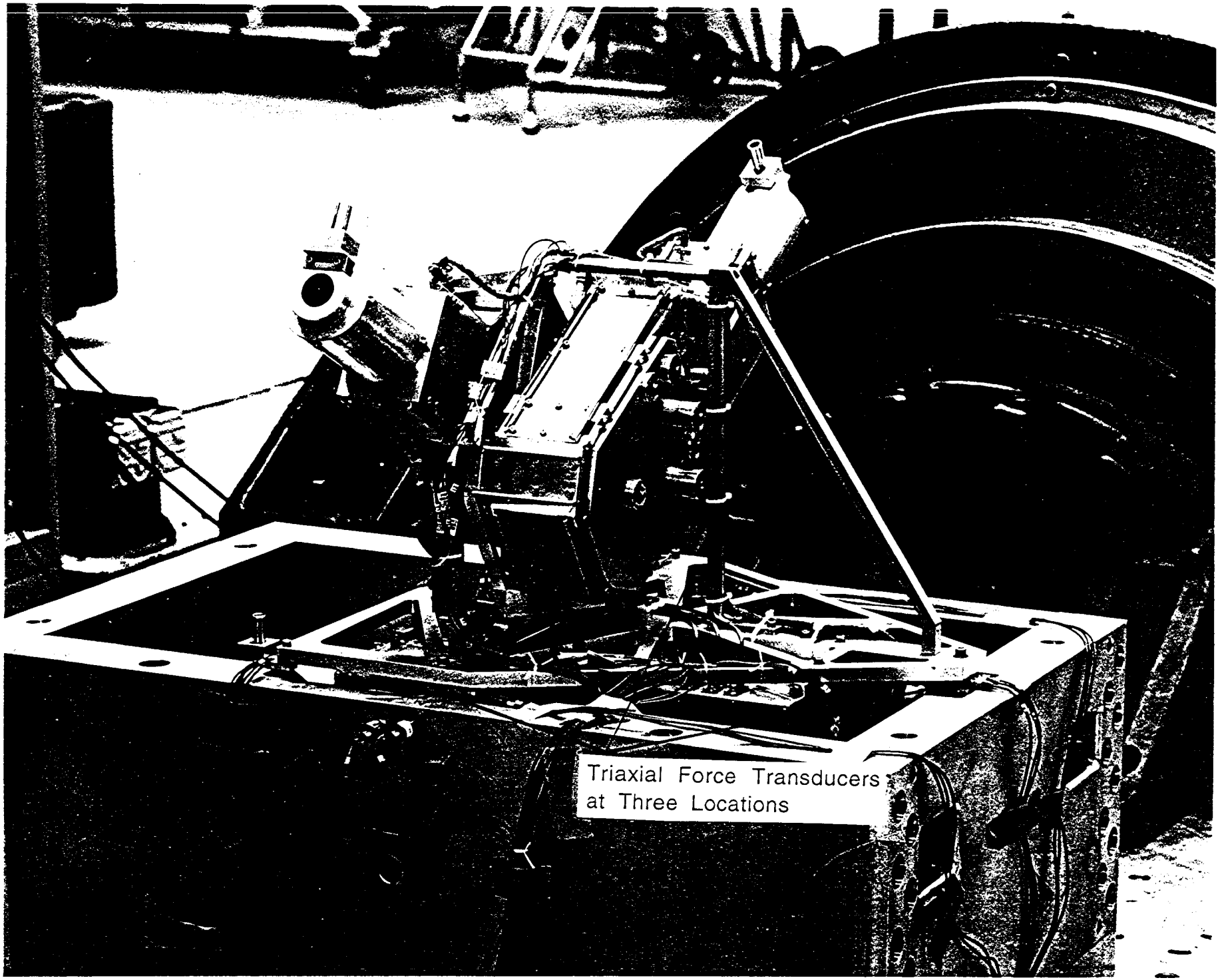
Triaxial Force Transducers
at Three Locations

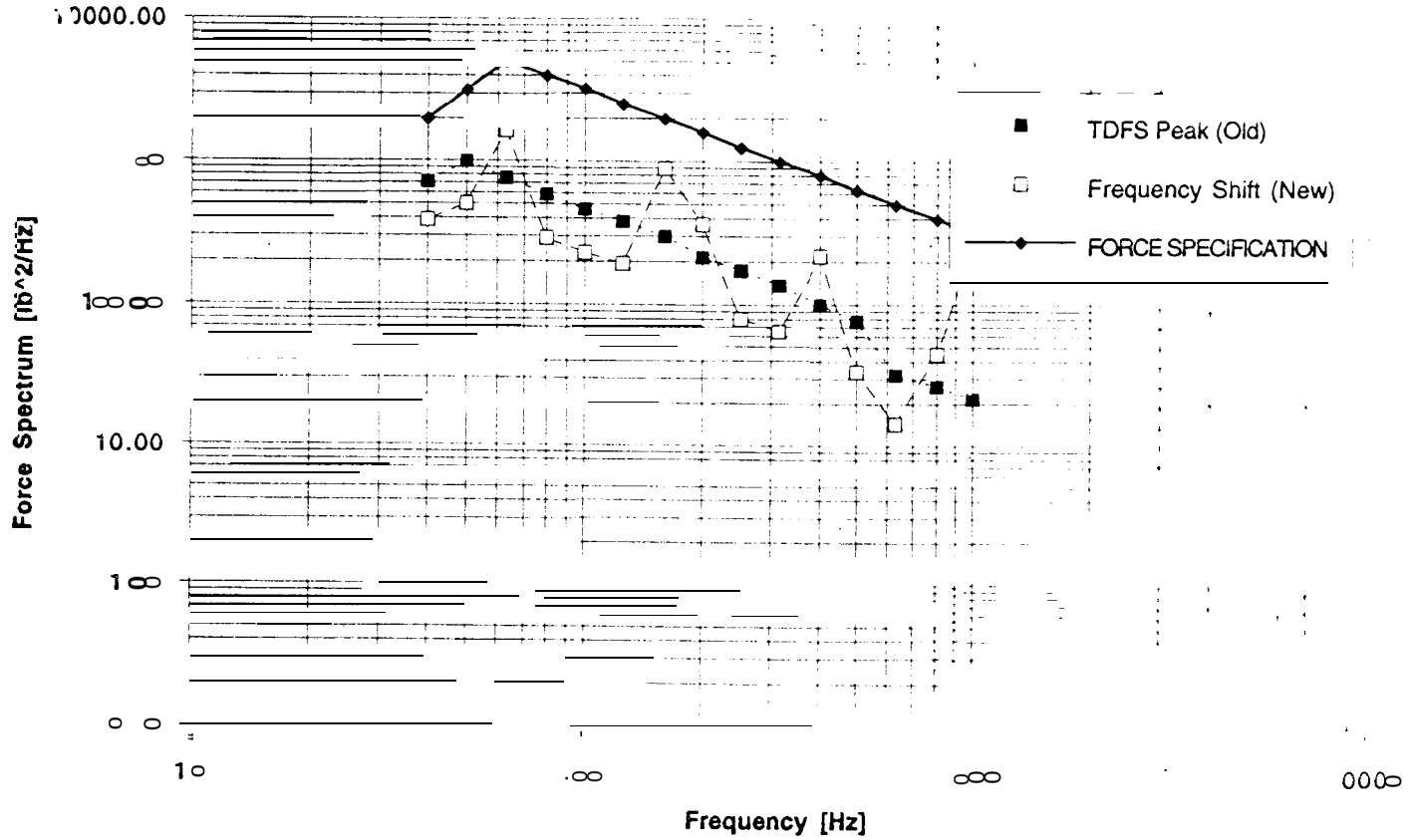
10000.00
1000
10.00
10
0 0
10
000
0000
Force Spectrum [lb^2/Hz]
Frequency [Hz]
TDFS Peak (Old)
Frequency Shift (New)
FORCE SPECIFICATION

PROJECT: CASSINI

TITLE: RPWS ANT ASSY

AXIS: X TEST DATE 4/13/94

PF - 18 dB

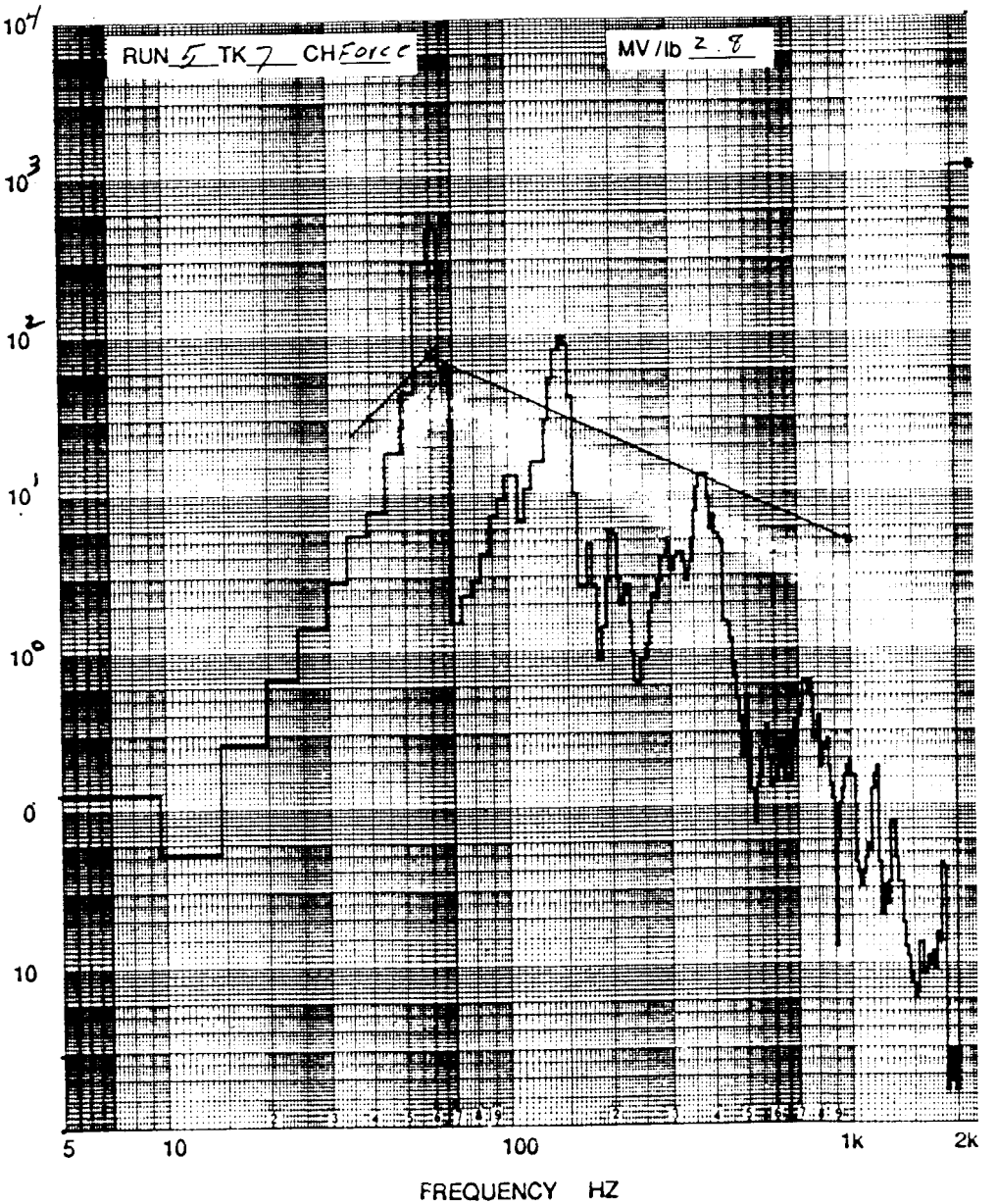

OA: 92.3 lb rms

ANALYSIS DATE____

PROJECT: CASSINI

TITLE: RPWS ANT ASSY

AXIS: X TEST DATE: 4/14/94

6dB W-FL

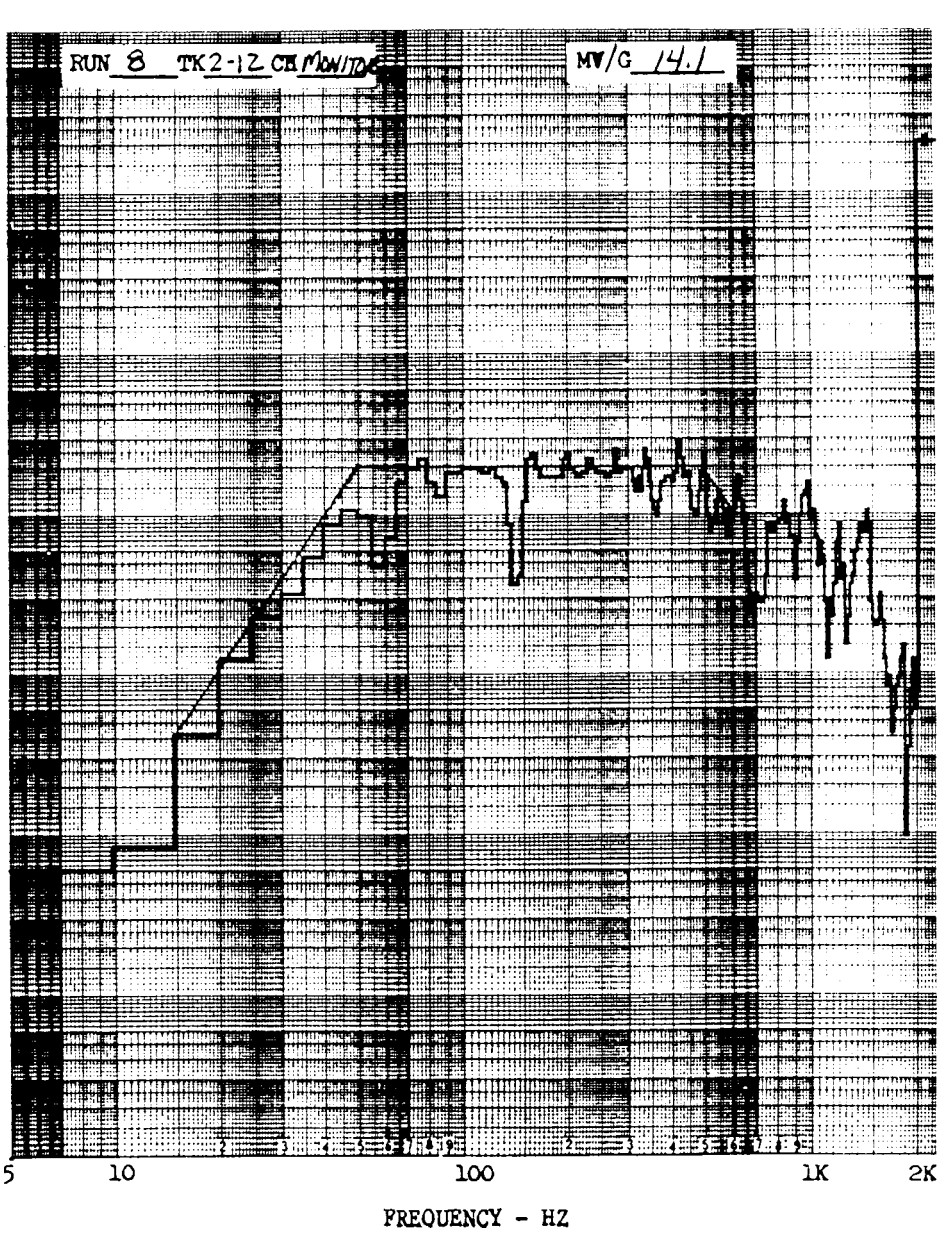

POWER SPECTRAL DENSITY - G^2/HZ

OA: 12.18 Grms

ANALYSIS DATE _____